Melting temperature of unrelaxed amorphous silicon

M. G. Grimaldi and P. Baeri
Dipartimento di Fisica, 57 Corso Italia, I95129, Catania, Italy

M. A. Malvezzi
Dipartimento di Elettronica, 209 via Abbiategrasso, I27100, Pavia, Italy
(Received 19 November 1990)

Direct picosecond laser measurements of the critical fluence for melting have been performed, showing unambiguously a 30% increase in the energy density required for surface melting of relaxed compared with unrelaxed amorphous silicon (*a*-Si). The difference in optical coupling cannot account for this variation, which can only be explained in terms of different melting temperatures. Heating of unrelaxed amorphous silicon samples at temperatures close to the melting point by nanosecond laser pulses produces, instead, relaxation of the amorphous phase. However, nanosecond uv irradiation of relaxed and unrelaxed amorphous silicon samples of various thicknesses has been used to determine the thermal conductivity and specific heat of the different amorphous states. Thermal conductivities of 4.8×10^{-3} and 6.5×10^{-3} W/cm K have been obtained for unrelaxed and relaxed *a*-Si, respectively, and a decrease of $\sim6\%$ in the specific heat of the amorphous phase upon relaxation has been determined. Using these data, the difference between the melting temperature of relaxed and unrelaxed amorphous Si has been derived to be 160 ± 50 K via picosecond data and 135 ± 15 K via free-energy calculations.

INTRODUCTION

Relaxation of amorphous silicon (*a*-Si) involves continuous evolution of the amorphous phase to a state of lower free energy following thermal treatment at temperatures lower than those required to induce crystallization. Changes in optical and structural properties of *a*-Si have been probed by infrared analysis,[1,2] Raman spectroscopy,[3] and x-ray diffraction.[4]

The heat of relaxation of ion implanted *a*-Si has been measured by calorimetric methods in the temperature range 400–950 K (Refs. 5 and 6) and it consists of two contributions: a homogeneous one due to relaxation of the amorphous phase (5.1 ± 1.2 kJ/mol) and an interfacial one due to crystallization of *a*-Si (13.4 ± 0.7 kJ/mol). Using the measured heat of crystallization and assuming a heat capacitance of the amorphous phase $\sim10\%$ higher than that of the crystal, the free energy curve of the relaxed *a*-Si phase relative to crystal silicon has been calculated with a melting temperature of 1420 K (Ref. 6), which is 265 K lower than that of crystal silicon. Moreover, adding the heat of relaxation to the heat of crystallization in the free-energy calculations, a 200 K reduction in the melting temperature of unrelaxed *a*-Si with respect to relaxed *a*-Si is expected.[6]

Contrary to these estimates, in a recent paper[7] we reported a difference between the experimental melting temperatures of relaxed and unrelaxed *a*-Si of 46 ± 12 K, a factor 4.5 lower. This value was obtained by measuring the energy threshold for surface melting of *a*-Si irradiated with 30-ns laser pulses at $\lambda=347$ nm and correcting for the measured difference in the product of the thermal conductivity k and specific heat c_p (a 24% increase upon relaxation) in the two cases. The reason for this discrepancy could be the occurrence of relaxation of *a*-Si during the heating induced by the laser pulse. In fact, laser-induced relaxation has been detected by Raman spectroscopy after irradiation of *a*-Si with 30-ns ruby laser pulses at energy densities just below the threshold for surface melting.[8] In a first attempt,[8] relaxation was attributed to the strong electronic excitation within the absorption length of the laser radiation. If this is the case, the melting temperature difference we measured is that of a partially relaxed to fully relaxed *a*-Si. On the other hand, if the laser pulse does not induce relaxation in *a*-Si, a change in the specific heat of *a*-Si following relaxation must be invoked to explain the previous data.

In this paper the differences in the surface melting threshold of relaxed and unrelaxed *a*-Si, measured by picosecond laser irradiation experiments, have been used to evaluate the differences in melting temperatures of the two states (see the section on picosecond irradiation). Further the results of nanosecond laser irradiation experiments on various types of *a*-Si samples have been used for a precise determination of thermal conductivity and specific heat in relaxed and unrelaxed amorphous silicon. These experiments are described in the section on nanosecond irradiation, while details of the data handling to calculate the thermal parameters can be found in the section on heat flow calculation. Finally, in the section on thermodynamical calculations, an estimate of the Gibbs free energy for both relaxed and unrelaxed *a*-Si has been deduced from the measured data.

EXPERIMENT

Amorphous silicon layers were produced by implantation at RT of Ge^+ ions into ⟨100⟩ Si crystal. The energies and doses of the ions were varied between 70–400 keV and 10^{14}–2×10^{15} cm^{-2}, respectively, so as to gen-

 ©1991 The American Physical Society

erate amorphous layers of different thicknesses. The implanted samples were annealed in a vacuum furnace (residual pressure $\sim 5\times10^{-7}$ torr) at 450 °C for 60 min to relax the amorphous structure and to remove the damaged layer at the crystal-amorphous interface. Part of the samples were successively derelaxed by reimplanting Ge ions at the same energy at a dose $\sim \frac{1}{10}$ of the previous one, since such a process results in a fully unrelaxed *a*-Si (Ref. 9). The thicknesses of the amorphous layers were in the range 70–350 nm as measured by Rutherford backscattering spectrometry of the 2.0-MeV He^+ incident along the ⟨100⟩ silicon direction.

Time-resolved reflectivity (TRR) measurements were used to detect the energy threshold for surface melting during laser irradiation. Two different lasers were used in the experiment: a 20-ps, frequency doubled, Nd:YAG ($\lambda=532$ nm) and a 30-ns, frequency doubled, ruby ($\lambda=347$ nm) laser.

The 20-ps pulsed laser had a Gaussian beam spatial profile. A low-intensity, 20-ps, $\lambda=1064$-nm pulse derived from the same laser and delayed 100 ps with respect to the pump pulse was used as a probe. In order to ensure laterally homogeneous heating conditions over the sampled surface, the ratio between pump and probe diameters was 10:1.

Due to multimode operation, the nanosecond laser pulse spatial profile was not smooth, and a uniformity of 10% over a circular area $\sim$2 mm in diameter was achieved by means of a bent quartz rod with a diffusing input end. The reflectivity was probed by a cw Ar laser ($\lambda=488$ nm) focused to a spot $\sim$500 μm in diameter in the center of the pump laser spot. The probe laser beam was polarized parallel to the incidence plane, and it was incident at a glancing angle on the sample surface so as to enhance the absolute difference between the signals of the light reflected by solid and liquid silicon.

Optical constants at the four wavelengths of interest were measured on our samples at room temperature by standard ellipsometric techniques.[10]

PICOSECOND LASER IRRADIATION

The infrared reflectivity measured $\sim$100 ps after irradiation with 20 ps, 532 nm in a 330-nm-thick relaxed (a) and unrelaxed (b) *a*-Si is reported in Fig. 1 as a function of the signal monitoring the energy density of the incident pump pulse. The linearity between the incident energy density and the monitor signal has been accurately checked; however, the absolute conversion is subject to large errors. A rough estimate based on comparison with crystalline Si samples indicates that the full abscissa scale correspond to an energy density of about 40 mJ/cm^2.

At low pump energy density the reflectivity has a constant value corresponding to that of solid amorphous silicon. Contrary to the case of *c*-Si, the reflectivity in this region does not show any particular feature versus laser fluence; therefore it has been fitted using a straight line.

By increasing the energy density of the pump pulse, a linear increase of the reflectivity signals is observed until saturation occurs at the liquid-silicon value. The transient behavior between solid- and liquid-silicon reflectivity results from the limited thickness of the liquid layer, which is smaller than the corresponding light extinction length in the liquid phase. Since an almost linear increase of the reflectivity signal with the molten thickness is expected in this case, we have fitted the data in the transient region using a straight line, as shown by the full lines in Fig. 1. The abscissa at the intersection between the two lines is assumed to correspond to the energy density threshold for surface melting E_{th}, and values of 0.79 ± 0.03 and 1.03 ± 0.02 V have been obtained by a fitting procedure for derelaxed and relaxed amorphous silicon, respectively. The corresponding ratio between the melting thresholds is $E_{th}^{rel}/E_{th}^{unr}=1.3\pm0.07$.

The ratio between the melting thresholds can be converted into the ratio of the melting temperatures, provided one knows the coupling parameters of the pump pulse

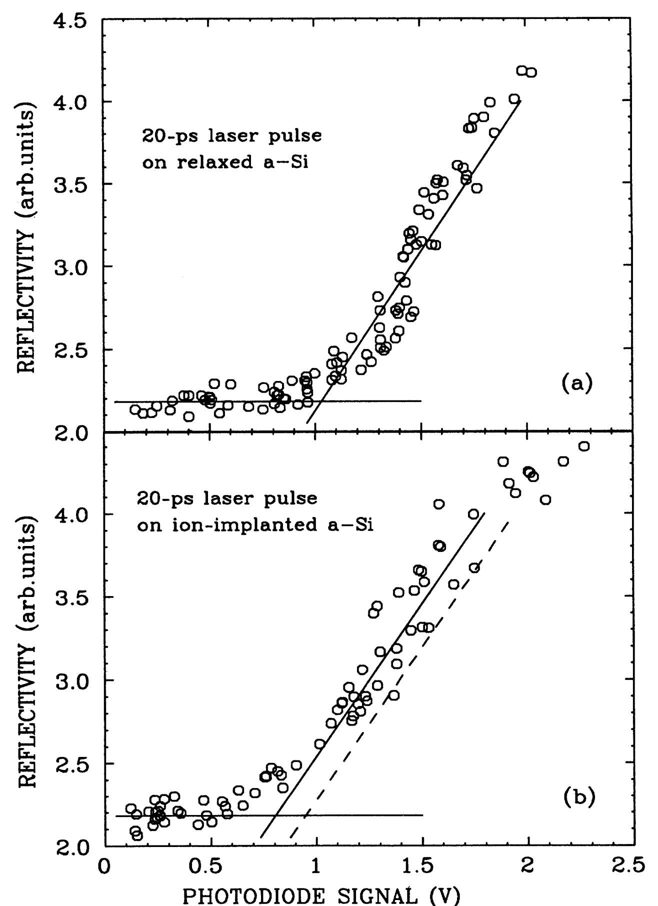

FIG. 1. Transient reflectivity at 1060 nm of *a*-Si samples measured $\sim$100 ps after irradiation with a 20-ps 532-nm pulse vs fluence. The full abscissa scale corresponds to $\sim$40 mJ/cm^2. (a) Results of a 330-nm-thick unrelaxed layer on a crystalline Si sample. (b) Results on a 330-nm-thick relaxed layer on a crystalline Si sample. The oblique dashed line corresponds to data from a 330-nm unrelaxed layer on a *c*-Si sample irradiated with a 347-nm, 25-ns laser pulse at a fluence just below that required to induce surface melting.

into the material. For this purpose accurate ellipsometry measurements were performed, and we obtained complex refractive indices at $\lambda=532$ nm of $4.709+i1.705$ and $4.631+i1.995$ for relaxed and derelaxed a-Si, respectively.

Heat-flow calculations, which will be discussed in detail below, have been performed using the previous data, and the ratio of the absolute melting temperature of a relaxed a-Si to that of an unrelaxed resulted in

$$\frac{T_M^{\mathrm{rel}}-T_R}{T_M^{\mathrm{unr}}-T_R}=1.17\pm0.06 ,$$

where T_R is the room temperature.

If we assume the melting temperature of relaxed a-Si to be 1420 K as computed in Ref. 6, the melting temperature of unrelaxed a-Si results in 1260 ± 50 K. The difference between two melting temperatures is then $T_M^{\mathrm{rel}}-T_M^{\mathrm{unr}}=160\pm50$ K.

To check whether relaxation occurs during nanosecond heating, we have measured, by picosecond irradiation, the melting threshold in unrelaxed a-Si previously irradiated with 347-nm nanosecond laser pulses at an energy density just below its melting threshold. The dashed oblique line in the lower part of Fig. 1 represents the fit of these reflectivity data points (not reported in the figure). The increase of the melting threshold with respect to the unrelaxed one supports the contention that the a-Si relaxed even in the nanosecond time scale. However, the uv irradiated sample does not appear fully relaxed, since a ratio of 1.2 ± 0.06 for the sample's melting threshold to that of the unrelaxed sample was obtained. This is somewhat below the one obtained in the case of the thermal relaxed-to-unrelaxed a-Si sample. The relaxation degree of a-Si can be probed by Raman spectroscopy.[3] We have performed, therefore, Raman analysis on the laser relaxed sample using a He-Ne laser ($\lambda=632.8$ nm) as a probe. We have no evidence of any significant relaxation. The last observations are consistent only if the thickness of the relaxed layer is much smaller (at least a factor of 5) than that probed by Raman measurements. The latter is of the order of the HeNe penetration depth (~100 nm), which, in turn, is comparable with the heat diffusion length during uv, ns pulsed irradiation. Therefore the laser-induced relaxation must be limited to a layer that is much smaller than the heated one, probably close to the uv light penetration depth (~10 nm). This is consistent with a model in which the laser-induced relaxation results from the strong electronic excitation along the laser absorption path disregarding the heating process itself.

NANOSECOND LASER IRRADIATION

The previously described experiments established the occurrence of a-Si relaxation during nanosecond laser irradiation. Therefore the difference in melting temperatures ($\Delta T=46\pm12$ K) deduced in Ref. 7 is that of a partially relaxed to a fully relaxed a-Si. In spite of that, nanosecond irradiation can still be used to investigate the thermal parameters of relaxed and unrelaxed a-Si. In fact the thickness of the layer relaxed by the laser pulse is much smaller than the heated one (~200 nm), so that the relaxed layer at the surface has almost no influence on the heating dynamics of the whole sample. In particular the increase of the product kc_p upon relaxation reported in the same Ref. 7 correctly describes the variation of this quantity on going from unrelaxed to fully relaxed a-Si.

In this section we will describe experiments in which nanosecond laser pulses ($\lambda=347$ nm, $\tau=25$ ns) have been used to determine both the specific heat and the thermal conductivity in thermally relaxed and unrelaxed a-Si. For this purpose the TRR technique was used to measure the energy density for surface melting of relaxed and unrelaxed amorphous silicon layers of different thicknesses x_a.

Great care has been taken to optimize and control the geometry as well as the electronics of the TRR apparatus. Measurements have been performed on different sets of samples, and the experimental accuracy in determining the ratio between melting thresholds by this method was always better than 0.5%.

In Fig. 2 the reflectivity measurements on relaxed a-Si samples of various thickness versus absorbed pump energy density are summarized. The samples are 330-nm-(○), 140-nm- (□), and 90-mm-(⌑) thick relaxed a-Si layers over crystalline substrates. Also in this case the linearity between the incident energy density and the monitor signal has been accurately checked, but only a rough estimate of the absolute energy density values was made, the full abscissa scale corresponding to ~100 mJ/cm^2. As in the case of picosecond laser irradiation the reflectivity increases continuously from the solid to the liquid-Si value near the melting threshold. However, unlike the picosecond irradiation case, the width of the fluence region between solid and liquid reflectivities cannot be justified entirely by interference effects due to the limited thick-

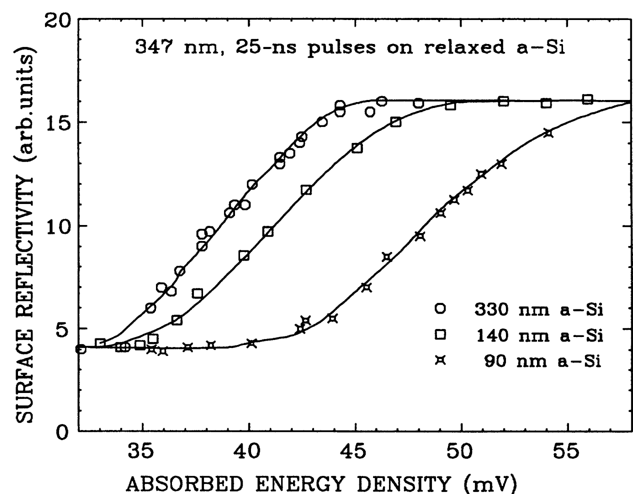

FIG. 2. Maximum reflectivity at 488 nm for relaxed a-Si samples of various thicknesses observed by time-resolved reflectivity (TRR) during excitation with a 347-nm, 30-ns laser pulses vs absorbed energy density (arbitrary units). The full abscissa scale corresponds to ~100 mJ/cm^2.

ness of the liquid layer. Instead, a nonhomogeneous surface melting due to the variation of the pump intensity over the probe spot explained the observed behavior. The position of melting threshold fluence is therefore assumed to be the energy density at which the reflectivity reaches a value halfway between solid and liquid silicon.

Figure 2 shows that an increase of the melting threshold occurs by decreasing the thickness of the a-Si layer. This behavior results from the lower thermal conductivity of the a-Si layer with respect to the crystalline bulk. The light extinction length α^{-1} in a-Si is much smaller than the thermal diffusion length $l=\sqrt{D\tau}$ ($D=k/\rho c_p$ being the diffusion coefficient, ρ the mass density, and τ the pulse duration); the latter, therefore, determines the temperature profile, and the absorbed energy is confined into the amorphous layer only if $x_a > l$. When $x_a \leq l$, heat can diffuse into the underlying crystal, which has a much greater heat conductivity, and the steeper temperature gradient generated at the amorphous-crystalline interface will drive heat out of the amorphous layer, thus increasing the energy required to reach the melting temperature at the sample surface. We found that the melting threshold was independent of the thickness of the amorphous layer if $x_a \geq 220$ nm.

Figure 3 shows the melting threshold energy density normalized to that of an infinitely thick amorphous layer (330 nm in our case) as a function of the amorphous thickness, circles referring to derelaxed and squares to relaxed a-Si. As shown in detail in the next section, this ratio depends only on the (average) value of the thermal diffusivity of a-Si, while it is independent of the precise value of the melting temperature. Data points clearly show a strong increase of the melting threshold when the

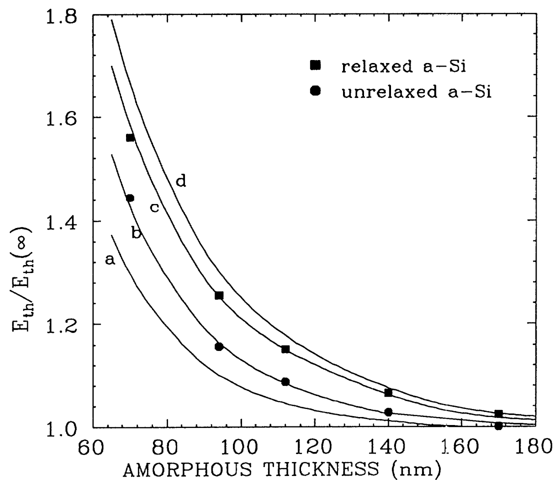

FIG. 3. Energy density for surface melting induced by nanosecond pulsed irradiation in a-Si layer of different thicknesses normalized to that of a 330-nm-thick a-Si as a function of the a-Si thickness. Data points for relaxed and unrelaxed a-Si are denoted by squares and circles, respectively. Full lines were calculated using the thermal model for different values of the parameter $k/\bar{c}_p$. (a) 3×10^{-3}, (b) 4.15×10^{-3}, (c) 5.9×10^{-3} and 7×10^{-3} g/cm s.

a-Si layer becomes thinner than 100 nm. Moreover, a greater variation of E_{th} with the a-Si thickness has been observed in the relaxed a-Si with respect to the unrelaxed one. As an example, the melting threshold measured in a 170-nm-thick relaxed a-Si was already 4% higher than that measured in the infinitely thick sample, while no difference was in evidence for an unrelaxed a-Si layer of the same thickness. The preceding data, therefore, indicate a greater thermal diffusion length for relaxed a-Si. The curves have been calculated using the heat-flow model with time-dependent thermal parameters, which will be described in the next paragraph. However, they can be obtained even using constant values for the thermal diffusion length l during the laser pulse. Fitting of the experimental data provided $l=1.0\times10^{-5}$ and 1.2×10^{-5} cm for the unrelaxed and relaxed amorphous a-Si, respectively.

HEAT-FLOW CALCULATIONS

The experimental laser fluences for surface melting discussed above will now be used in heat-flow calculations in order to deduce melting temperatures of relaxed and unrelaxed amorphous silicon. The basic processes in laser irradiation and surface melting of solid absorbing target are heat generation and cooling by heat conduction into the substrate. The absorbed light is instantaneously converted into heat, which diffuses according to heat flow. Most of the features of such a process can be predicted by solving the heat diffusion equation with a source term that describes the laser heating and with the appropriate boundary conditions to account for phase transformations and sample geometry.[11]

In the following the correlation between the thermal properties c_p, k and melting temperature T_M of the irradiated material and the melting threshold E_{th} will be emphasized. Numerical solutions of the heat-flow equation are required to account for the temperature dependence of all thermal and optical parameters. However, to get an immediate feeling of the relevance of these parameters on the melting threshold evaluation, we report in the Appendix the approximate analytical solutions of the heat-flow equation for these cases whose numerical solution is discussed below.

Numerical heat-flow calculations[11] have been performed using temperature-dependent thermal and optical parameters for both amorphous and crystalline silicon. Standard thermal[12] and optical[13] parameters were used for the Si substrate.

For nanosecond uv pulsed experiments, a reflectivity $R=0.525$ and an absorption coefficient $\alpha=1\times10^{6}$ cm^{-1} at $\lambda=347$ nm for both relaxed and unrelaxed a-Si were measured by ellipsometry and used in the calculations. Values in the range $3-8\times10^{-3}$ W/cm K for the thermal conductivity were adopted in the calculations. These values, deduced from previous experiments,[14] are typical of glass materials. The thermal conductivity of such materials exhibits a very weak temperature dependence[15] and therefore it has been assumed constant at $T > T_R$.

The specific heat of a-Si has never been measured but a scaling[16] of the data for a-Ge (Ref. 17) suggests that at

high temperatures c_p should be $\sim 10\%$ higher in relaxed a-Si with respect to crystal Si. The following expression for c_p has then been used in the calculations[6,16] (in units of J/g K)

$$c_p^a(T) = c_p^{\rm xtal}(T) + \gamma \left[-7.97\times 10^{-3} + 0.17 \times \frac{T}{1685} \right] , \quad (1)$$

where $c_p^{\rm xtal}(T) = 0.81 + 1.3\times 10^{-4}T - 1.26\times 10^4 T^{-2}$ is the specific heat of crystalline silicon, T is the temperature in Kelvin, and the second term is a correction to account for the higher specific heat of a-Si. The value $\gamma = 1$ has been used in Refs. 6 and 16, and it gives an a-Si specific heat that corresponds to that obtained by scaling the a-Ge value for the different melting temperature. We used γ as a fitting parameter, which in our calculations was varied between 1 and 3. The specific heat averaged over the temperature range from T_R to T_M is roughly equal to $\bar{c}_p \simeq (1+\gamma/10)$ (J/g K).

Numerical solutions of the heat-flow equation performed for an infinitely thick a-Si layer irradiated with uv, ns laser pulses are shown in Fig. 4(a) where the maximum surface temperature is reported as a function of the input energy density for different values of k and γ. The calculated temperatures for different k and γ values were equal within 0.5% provided that the product $\sqrt{k\bar{c}_p}$ remains constant. The same result has been obtained analytically assuming constant thermal parameters as reported in the Appendix. By fixing a given value for the melting temperature of a-Si, one can then plot the laser fluence as a function of quantity $\sqrt{k\bar{c}_p}$, as illustrated in Fig. 4(b). The linear dependence in the plot indicates again that using constant material parameters deduced by averaging over the expected temperature range is indeed a good approximation in the case of nanosecond interaction. In particular, due to this linearity, ratios of the melting fluences turn out to be independent from melting temperatures. The ratio of the melting thresholds of a sample with an infinitely thin unrelaxed layer over a 330-nm relaxed a-Si layer to one made of a full 330-nm unrelaxed a-Si layer has been determined experimentally[7] in 1.115 ± 0.005. From Fig. 4(b) therefore, a relation between the quantities $\sqrt{k\bar{c}_p}$ for the two states of a-Si may be deduced:

$$(\sqrt{k\bar{c}_p})_{\rm rel} = (1.129\pm 0.005)(\sqrt{k\bar{c}_p})_{\rm unr} . \quad (2)$$

The experimental data of Fig. 3 may then provide an additional relation between γ and k in the two states of a-Si. In this case, one has to simulate samples with different layers of amorphous over crystalline substrates. The results of the simulations do not show appreciable change when the value of γ and k are changed so as to keep the value of $\bar{D} = k/\rho\bar{c}_p$ constant. Again, as shown in the Appendix, this result indicates that approximate solutions of the heat-flow equation may be expressed in terms of the average diffusion coefficient $\bar{D}$. The fit of the experimental data, indicated by the solid lines in Fig. 3, provides the following relation (in units of g/s cm):

$$\left[\frac{k}{\bar{c}_p} \right]_{\rm rel} = (5.90\pm 0.05)\times 10^{-3} , \quad (3a)$$

$$\left[\frac{k}{\bar{c}_p} \right]_{\rm unr} = (4.15\pm 0.05)\times 10^{-3} . \quad (3b)$$

Since for relaxed a-Si $\gamma_{\rm rel} = 1$, we obtain from Eqs. (1) and (3a) $k_{\rm rel} = (6.5\pm 0.066)\times 10^{-3}$ W/cm K. Coupling Eqs. (1), (2), and (3b), the absolute values of the thermal conductivity and γ can be obtained for the unrelaxed a-Si too: $k_{\rm unr} = (4.82\pm 0.15)\times 10^{-3}$ W/cm K, $\gamma_{\rm unr} = 1.63 \pm 0.16$.

Once the heat transport parameters are known for both relaxed and unrelaxed a-Si, complete numerical cal-

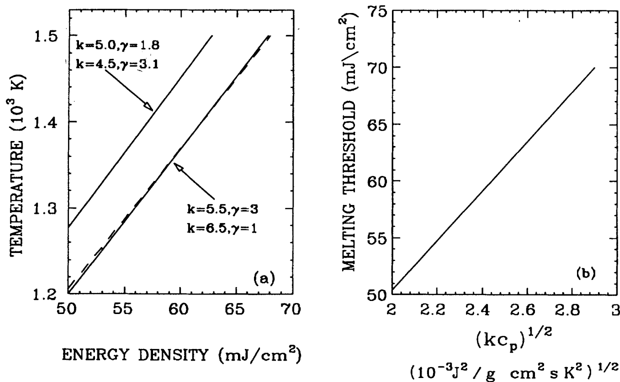

FIG. 4. Heat-flow calculations for a 347-nm, 30-ns laser heating pulse impinging onto 330-nm-thick a-Si targets. (a) Maximum surface temperature vs pump laser energy density for different values of thermal conductivity k and fitting parameter γ. k values are in units of 10^{-3} W/cm K. (b) Threshold laser energy density for melting vs product $(k\bar{c}_p)^{1/2}$ assuming a melting temperature $T_M = 1420$ K.

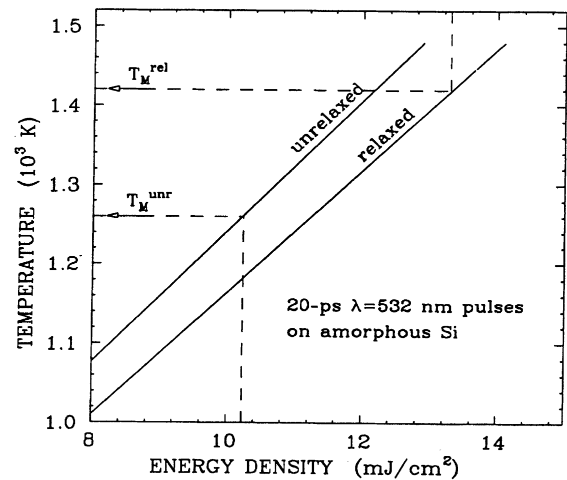

FIG. 5. Heat-flow calculations for 532-nm, 20-ps laser heating pulse impinging onto a-Si targets. Calculated temperature vs pump energy density for relaxed and unrelaxed bulk a-Si samples.

culations can be performed for picosecond irradiation. The maximum surface temperature calculated as a function of the energy density of 20 ps, 532-nm laser pulses is reported in Fig. 5 for 330-nm-thick layers of relaxed and unrelaxed a-Si. Two different curves have been obtained for relaxed and unrelaxed a-Si because of their different specific heat and optical parameters. Deviations of the calculations from the analytical solution given in Eq. (3) are mainly due to the not completely negligible heat diffusion length and are within 5% anyway. Unfortunately our absolute energy calibration is not accurate enough to determine the absolute value of the melting temperature from these data. However, assuming 1420 K for the relaxed a-Si melting temperature,[6] the measured ratio between the melting thresholds in the picosecond irradiation experiment results in a melting temperature of 1260±50 K for the unrelaxed a-Si.

THERMODYNAMICAL CALCULATIONS

The evaluation of the specific heat of both relaxed and unrelaxed a-Si allows the calculation of the relative Gibbs free energy of these states. In Ref. 15 Donovan has calculated the free energy of the relaxed amorphous referred to the crystalline phase

$$\Delta G_{ac}(T)=\Delta H(T_0)+\int_{T_0}^{T}\Delta c_p\,dT-S_a T-T\int_0^T\frac{\Delta c_p}{T}\,dT\ ,$$

where $\Delta c_p = c_p^a(T) - C_p^{\mathrm{xtal}}(T)$ is obtained from Eq. (1) using $\gamma=1$, S_a is the zero-point entropy, which has been estimated in Ref. 17 on the basis of the structural configuration of the amorphous network to be 1.66 J/mol K, and $\Delta H(T_0)$ is the crystallization enthalpy measured at temperature $T_0=950$ K by differential scanning calorimetry (DSC). The result of this calculation is shown in Fig. 6 (curve labeled relaxed).

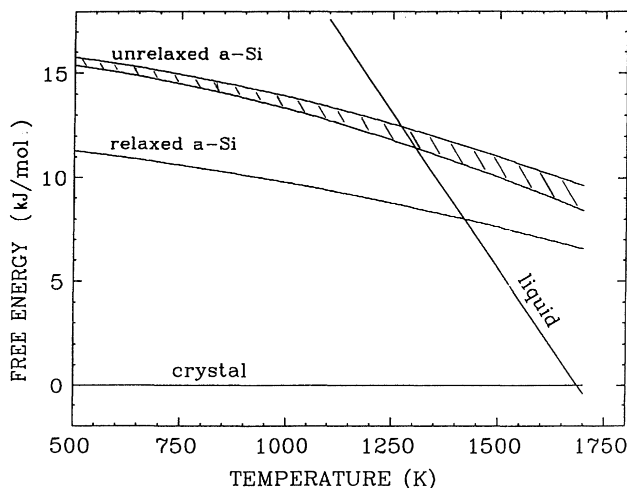

FIG. 6. Free energy of relaxed and unrelaxed amorphous silicon referred to crystal silicon vs temperature. The shaded region represents the lack of determination in the unrelaxed free-energy curve resulting from the error in our c_p^{unr} determination.

In order to calculate the free-energy curve for the unrelaxed amorphous a-Si we used the specific heat deduced in our nanosecond heating experiment, i.e., the one corresponding to $\gamma=1.63\pm0.16$; $\Delta H(T_0)$ was assumed to be the sum of the crystallization and relaxation enthalpy reported in Ref. 6. The results of the calculation are also shown in Fig. 6 (curve labeled unrelaxed). The shaded area represents the indetermination deriving from the error in the γ value. From these curves a melting temperature of 1285±15 K for the unrelaxed a-Si is evaluated. The zero-point entropy calculated in Ref. 18 did not take into account the presence of defects in the random network. Recent measurements indicated that the defect density in fully unrelaxed a-Si corresponds to 7% displaced atoms, which annihilate upon relaxation.[19] The presence of defects results in a slightly higher zero-point entropy for the unrelaxed state. We have estimated $S_0=2.16$ J/mol K as the upper limit. Using this last value the evaluated melting temperature increases to 20 K. Assuming identical thermal parameters for the relaxed and unrelaxed states, a melting temperature of 1220 K for the unrelaxed has been instead evaluated in Ref. 6.

SUMMARY AND CONCLUSION

Pulsed laser heating of relaxed and unrelaxed a-Si samples has been used to evaluate the melting temperatures. Relaxation of the amorphous phase has been observed to occur in a layer of the order of light absorption length from the sample surface during interaction with nanosecond laser pulses. Faster heating is then required to perform measurements unaffected by the ongoing relaxation process. Using picosecond laser pulses, the measured ratio of threshold fluence for melting relaxed a-Si to that for melting an unrelaxed sample is 1.3 ± 0.7. Precise knowledge of thermal and optical parameters of relaxed and unrelaxed a-Si is then necessary to transform this result into the ratio between the melting temperatures. Nanosecond laser pulses have been used to determine the thermal conductance and specific heat of the different amorphous states. A thermal conductivity of 4.8×10^{-3} and 6.5×10^{-3} W/cm K has been obtained for unrelaxed and relaxed a-Si, respectively, and a decrease of $\sim6\%$ in the specific heat of the amorphous phase upon relaxation has been determined.

With the knowledge of the thermal parameters of the a-Si states, melting temperatures of a-Si have been determined using two independent methods. From the picosecond irradiation results, and assuming a melting temperature of 1420 K for the relaxed a-Si, we have calculated the melting temperature of the unrelaxed state to be 1260±50 K.

The second method relies on the calculation of the free energy of the two amorphous states using the enthalpy measured in Ref. 6 and the present determination of the specific heat. In this way a melting temperature of 1420 and of 1285±15 K for the relaxed and unrelaxed a-Si, respectively, has been obtained.

The melting temperatures determined by the two different approaches coincide within the experimental errors. It should be noted also that the error in γ (and

therefore the error in c_p) affects our ΔT_M determination in opposite ways in the two methods. In fact, the difference between the melting temperatures of relaxed and unrelaxed *a*-Si determined by picosecond irradiation experiments increases with increasing γ, just the opposite of that determined from the free-energy diagram for which a decrease of ΔT_M is observed with increasing γ. For example, $\gamma=1$ and 2 results in $\Delta T_M=130$ and 180 ± 50 K, respectively, when picosecond laser data are used, while the same variation of γ results in $\Delta T_M=200$ and 80 K when the thermodynamical approach is followed. Our determination of the specific heat of unrelaxed *a*-Si is therefore the only one that gives a value of ΔT_M, which is consistent with the two approaches.

The last remark can be made on the reasons why picosecond laser irradiation, unlike the nanosecond case, does not induce relaxation in *a*-Si. Two main differences are relevant. The first one is the lower density of absorbed photons in picosecond irradiation with respect to nanosecond pulses. In fact, a melting threshold of ~ 15 mJ/cm^2 and of ~ 70 mJ/cm^2 has been measured in a 330-nm-thick *a*-Si by picosecond and nanosecond pulsed irradiation, respectively; taking into account the different absorption coefficients at the two wavelengths, one can estimate a difference of about a factor 20 in the density of the absorbed photons. The second one is the different heating time scale. Relaxation of *a*-Si during fast heating probably results from both a thermally activated process and electronic excitation; therefore, the reduced time duration of the whole process during picosecond irradiation may inhibit the relaxation process occurring, instead, during nanosecond pulsed heating. In Ref. 4 it has been shown that ion beam derelaxation of *a*-Si depends on nuclear not electronic processes. This would seem to show that fast electronic processes are unimportant in the relaxation of *a*-Si. It should be noted, however, that the electronic excitation generated inside the single-ion track decays in a very short time (≤ 1 ps), and therefore these processes are most like those occurring during picosecond irradiation, where no relaxation was observed. Moreover in that particular experiment the substrate was kept at LN_2 temperature. The different experimental results are therefore not surprising and a characterization of the role of electronic excitation on *a*-Si relaxation by *e* beam and laser irradiation will be required to compare the different experiments.

ACKNOWLEDGMENTS

We would like to thank G. Reverberi and R. Reitano for ellipsometric measurements and N. Marino for assistance with the laser equipment.

APPENDIX

Assuming optical and thermal material parameters independent from temperature, an estimate of the laser fluence necessary for melting the surface of bulk samples with nanosecond pulses may be derived simply by energy balance considerations. When the radiation absorption length α^{-1} is much less than the thermal diffusion length of the material $\sqrt{D\tau}$ with $D=k/\rho c_p$, the energy of the laser pulse is released in a thickness $\sqrt{D\tau}$ and a maximum increase of the temperature from T_R to T_M is observed. Here, α is the absorption coefficient of the laser radiation, ρ is the density, c_p the specific heat of the material, and τ the laser pulse duration. The following approximate relation then holds:

$$(1-R)E_{\text{th}}=\frac{\sqrt{\pi}}{2}\sqrt{kc_p}\sqrt{\rho\tau}(T_M-T_R)\ , \tag{A1}$$

where R is the sample reflectivity, E_{th} the threshold laser energy density (J/cm^2) for surface melting, T_M the melting temperature, and T_R the room temperature. This equation holds for bulk samples, and also in the case of samples with an extremely thin layer (less than one tenth of the diffusion length $\sqrt{D\tau}$) of different material near the surface, provided the melting temperature T_M refers to the film melting point and the thermal parameters to the bulk material. Equation (A1) thus states that the temperature rise is proportional to laser energy density. In particular, for a given melting temperature the threshold energy density is proportional to $\sqrt{kc_p}$.

When an amorphous layer of thickness x_a comparable with $\sqrt{D\tau}$ is considered over a crystalline bulk substrate, Eq. (A1) has to be modified in order to take into account the greater diffusion coefficient of the crystal as compared to the one of the amorphous layer. The fraction of the energy that reaches the amorphous-crystal interface during the laser pulse is diluted into the substrate and, in a first approximation, it is not more available for the heating process. The energy fraction retained in the amorphous layer is roughly equal to the ratio of the thermal diffusion time through the amorphous layer (x_a^2/D_a) to the pulse duration, being D_a the diffusion coefficient of the amorphous material. As a result, the energy balance equation reads in this case:

$$(1-R)E_{\text{th}}\frac{x_a^2}{D_a\tau}=\rho c_p x_a(T_M-T_R)\ . \tag{A2}$$

The ratio of the threshold energy density for a sample of amorphous thickness x_a to one with infinite amorphous thickness then may be evaluated from Eqs. (A1) and (A2) in

$$\frac{E_{\text{th}}(x_a)}{E_{\text{th}}(\infty)}\simeq\frac{x_a}{\sqrt{D_a\tau}}\ . \tag{A3}$$

The ratio of the threshold energy densities is then, under these simple assumptions, independent of the melting temperatures.

Finally when the heat diffusion length during the laser pulse is smaller than the light penetration depth, as is the case in picosecond laser irradiation experiments, the actual value of the thermal conductivity becomes less important in determining the melting threshold which in turns, for infinitely low thermal conductivity k, depends only on the absorption coefficient. The following approximate equation then holds:

$$(1-R)E_{\text{th}}\simeq c_p\alpha^{-1}(T_M-T_R)\ . \tag{A4}$$

[1]P. Baeri, A. E. Barbarino, S. U. Campisano, M. G. Grimaldi, G. Foti, and E. Rimini, in *Laser and Electron-Beam Interactions with Solids,* edited by B. R. Appleton and G. K. Celler (Elsevier, Amsterdam, 1982), p. 227.
[2]J. E. Fredrickson, C. N. Waddel, W. G. Spitzer, and G. K. Hubler, Appl. Phys. Lett. **40**, 172 (1982).
[3]R. Tsu, J. G. Hernandez, and F. H. Pollak, J. Non-Cryst. Solids **66**, 109 (1984).
[4]S. Roorda, W. C. Sinke, J. M. Poate, D. C. Jacobson, P. Fuoss, B. S. Dennis, S. Dierker, and F. Spaepen, Proc. Mater. Res. Soc. **157**, 683 (1990).
[5]S. Roorda, S. Doorn, W. C. Sinke, P. M. Scholte, and E. van Loenen, Phys. Rev. Lett. **62**, 1880 (1989).
[6]E. P. Donovan, F. Spaepen, J. M. Poate, and D. C. Jacobson, Appl. Phys. Lett. **55**, 1516 (1989).
[7]M. G. Grimaldi and P. Baeri, Appl. Pjhys. Lett. **57**, 614 (1990).
[8]W. Sinke, T. Warabisako, M. Miyao, T. Tokuyama, S. Roorda, and F. W. Saris, J. Non-Cryst. Solids **99**, 308 (1988).
[9]S. Roorda, W. C. Sinke, J. M. Poate, S. Dierker, B. S. Dennis, D. J. Eaglesham, and F. Spaepen, Proc. Mater. Res. Soc. **157**, 709 (1990).
[10]R. M. Azzam and N. M. Bashara, in *Ellipsometry and Polarized Light* (North-Holland, Amsterdam, 1987).
[11]P. Baeri and S. U. Campisano, in *Laser Annealing of Semiconductors,* edited by J. M. Poate and J. W. Mayer (Academic, New York, 1982), Chap. 4.
[12]A. Goldsmith, T. Waterman, and H. Hirschorn, *Handbook of Thermophysical Properties of Solid Materials* (Macmillan, New York, 1961), Vol. I.
[13]D. E. Aspnes and A. A. Studna, Phys. Rev. B **27**, 985 (1983).
[14]M. G. Grimaldi, P. Baeri, and G. Baratta, Proc. Mater. Res. Soc. **157**, 419 (1990).
[15]D. G. Cahill, H. E. Fischer, T. Klitsner, E. T. Swartz, and R. O. Pohl, J. Vac. Sci. Technol. A **7**, 1259 (1989).
[16]E.P. Donovan, F. Spaepen, D. Turnbull, J. M. Poate, and D. C. Jacobson, J. Appl. Phys. **57**, (1985).
[17]H. S. Chen and D. Turnbull, J. Appl. Phys. **40**, 4214 (1969).
[18]F. Spaepen, Philos. Mag. **30**, 417 (1974).
[19]S. Roorda, J. S. Custer, W. C. Sinke, J. M. Poate, D. C. Jacobson, A. Polman, and F. Spaepen, Nucl. Instrum. Methods (to be published).